Sawtooth Signal Generator Using a Carbon-Based Memristor

Ertugrul KARAKULAK[1], * 　, Resat MUTLU[2]

[1] Electronics Department, Vocational School of Technical Sciences, Tekirdağ Namık Kemal University, Tekirdağ, Türkiye
[2] Electronics and Communication Engineering Dep, Çorlu Engineering Faculty, Tekirdağ Namık Kemal University, Çorlu, Tekirdağ, Türkiye

Highlights
• This paper focuses on a memristor-based sawtooth signal generators.
• A new application area for the Self-Directed Channel (SDC) Carbon-based Memristors is suggested.
• The performance of the signal generator has been examined with simulations and experimentally.

Article Info

Abstract

It is possible to use the new electronic circuit element memristor in analog applications. Memristors or memristor emulators have already been applied in analog applications such as amplifiers, filters, oscillators, and chaotic circuits. In literature, it has been recently demonstrated that a memristor-based sawtooth signal generator can be built utilizing a memristor emulator and simulations with various memristor models. Such a sawtooth signal generator needs experimental verification with a memristor. Self-Directed Channel (SDC) Carbon-based Memristors are in the market now. Once, the memristor technology is mature enough, its applications may also follow soon. Any memristor application should be realized with a memristor, not an emulator. Knowm memristor has not been used to design a sawtooth signal generator in the literature previously. The aim of the study is to show that a sawtooth signal generator can be made using a Self-Directed Channel (SDC) Carbon-based Memristor and to examine it experimentally. The performance of this sawtooth signal generator is evaluated. The waveforms of the proposed circuit are also examined by varying its operating frequency. The simulation and experimental results are compared. It has been found that its waveforms can be predicted well up to 350 kHz and its high-frequency behavior is not predicted well above 350 kHz by the memristor model used.

1. INTRODUCTION

A memristor is a nonlinear circuit element that has been envisioned in [1]. The resistance or memristance of an ideal memristor does depend on its charge which is equal to the integral of its current in the time domain. That's why it has a memory, i.e., it remembers its resistance when its supply is cut off. Memristive systems which possess similar characteristics to memristors have been defined in [2]. A thin-film TiO_2 memristive system placed between Platinum contacts is demonstrated to act as if it were a memristor for some of its operation range [3,4]. Memristive systems and memristors have become hot research areas nowadays. Some reviews on memristor and memristive systems are given in [5-9]. Most of the work on memristors has focused on making memristors, investigating memristive materials, making memristor emulators, and theoretical studies in which researchers are trying to figure out how to use memristors in the best way possible or find new application areas [5-9]. Analog application areas of memristors are also currently a hot topic [8], [10-13]. In 1971, even when the memristor was only a speculative circuit element, Chua predicted that a memristor-based staircase signal generator application might be possible [1]. In [1], It has been claimed that oscillators that cannot be made using traditional circuit components could have been made with it. It may be possible to adjust not only frequencies but also threshold parameters automatically in memristor-based oscillators [10,14]. It is possible to make reactance-less oscillators with memristors [15-18]. Memristor-based Duffing oscillators and their dynamics are examined in [19-21]. Memristor-based relaxation oscillators are examined in [10,22-24]. Some of the memristor applications have focused on the Wien-bridge oscillators [25-29]. In [30], it is demonstrated that a memristor-based sawtooth signal generator (MBSSG) can be built. In [30], the HP memristor model is used to simulate the

MBSSG, and an HP memristor emulator is used in the experiments to prove the concept. The MBSSG is inspected using several memristor models and with the Simulink^{TM} toolbox of the Matlab^{TM} program [31]. Memristor models are not mature enough. That's why any memristor application requires experimental verification of its performance. Knowm company has already started selling DIP packaged memristors [32]. It is expected that in the future more companies may produce memristors sold in the market [33]. A Knowm memristor is used to demonstrate chaos experimentally [34]. To the best of our knowledge, a Carbon-based Knowm memristor has not been used in such a sawtooth signal generator in the literature, yet. In this study, an MBSSG is made using a carbon-based memristor produced by Knowm company for the first time in the literature [31], its performance is examined with simulations and experimentally, and its frequency response is also studied. The MBSSG is simulated with the Biolek memristor model. The simulation and the experimental results are compared to each other.

The study is structured as follows. In the second section, basic information on the Self-Directed Channel (SDC) Carbon-based memristor is given. In the third section, the MBSSG is briefly explained, and its simulations are presented. The experimental results of the MBSSG are given in the fourth section. The study is concluded with the last section.

2. SELF DIRECTED CHANNEL (SDC) CARBON-BASED MEMRISTOR

The Knowm Self-directed channel (SDC) memristor material pack, which is a metal ion-conducting device often referred to as an electrochemical metallization cell (ECM), depends on Ag+ movement into channels within the active layer to change the device memristance. The carbon-based memristor topologies are shown in Figure 1 [32]. Dopants such as W, SN, CR, and C are used for improving and optimizing of Knowm memristor properties therein. More information about Knowm memristors can be found in [32].

The Knowm memristors have a 16-pin ceramic DIP package [32]. It contains 8 memristors. Hysteresis curves of a memristor are obtained under AC excitation and usually, sinusoidal signals are used for this purpose. One of the Carbon-based Knowm memristors is excited with a sinusoidal wave and its zero-crossing pinched hysteresis curves for 1 and 10 kHz can be seen in Figure 2 to illustrate its memristive behavior. With increasing frequency, the area of the zero-crossing hysteresis loop shrinks which is a fingerprint of memristive systems [35].

Figure 1. *SDC material stack [32]*

(a)   *(b)*

Figure 2. *Hysteresis loops of a Carbon-based memristor under sinusoidal excitation for a)1 kHz and b)10 kHz*

3. THE MEMRISTOR-BASED SAWTOOTH SIGNAL GENERATOR AND ITS SIMULATION

The MBSSG circuit given in [30] is shown in Figure 3. The Knowm memristor symbol given in [32] is not used in this study. Chua's memristor symbol is preferred and used in the MBSSG circuit since it is well-known. The generator consists of an opamp-based relaxation oscillator (OBRA) and a memristor-based inverting amplifier (MBIA) as seen in Figure 3. The OBRA provides the needed square waveform. Resistor-Memristor (R-M) inverting amplifier examined in [36]. The memristance or the resistance of the Knowm memristor increases for the current direction given in Figure 3. The series resistor Rs seen in Figure 3 has been used to protect the Knowm memristor as suggested in [32].
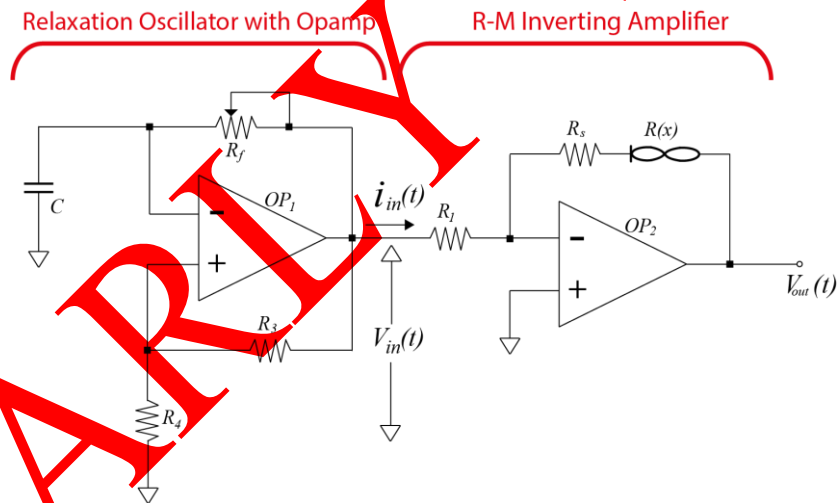

Figure 3. *The MBSSG circuit [30]*

The output voltage of the OBRA is equal to the input voltage of the MBIA. The voltage is written as the following piecewise function:

$$V_{in} = \begin{cases} V_{sat}, & 0 < t < \frac{T}{2} \\ -V_{sat}, & \frac{T}{2} < t < T \end{cases} \tag{1}$$

where T is the electrical period and V_{sat} is the magnitude of the voltage of the OBRA. The frequency of the relaxation oscillator is equal to

$$f = \frac{1}{2ln(3)RC} \tag{2}$$

The input current of the MBIA;

$$I_{in} = \frac{V_{in}}{R_1} = \begin{cases} \frac{V_{sat}}{R_1}, & 0 < t < \frac{T}{2} \\ -\frac{V_{sat}}{R_1}, & \frac{T}{2} < t < T \end{cases} \tag{3}$$

where R_s is the resistance of the protection resistor and R_1 is the input resistance of the MBIA. A memristor model with nonlinear dopant drift is described as

$$v(t) = R(x)i(t) \tag{4}$$

$$\frac{dx}{dt} = \frac{\mu_v R_{on}}{D^2} i(t) f(x) \tag{5}$$

where D is the total length of the memristor layers, μ_v is the dopant mobility, $v(t)$ is the memristor voltage, $i(t)$ is the memristor current, $R(x)$ is the memristor memristance, w is the oxidized length of memristor, $x = \frac{w}{D}$ is the normalized oxidized length of memristor, $f(x)$ is the memristor's window function, and R_{ON} is the minimum memristance of the memristor. The memristance of the memristor can be given as

$$R(x) = R_{OFF} - (R_{OFF} - R_{ON})x \tag{6}$$

where R_{OFF} is the memristor's maximum memristance.
$x(t)$ ranges from 0 to 1. Therefore,

$$R_{ON} \leq R(x) \leq R_{OFF} \tag{7}$$

A window function is a measure of how close a memristor gets to being an ideal memristor. *p* modifies the shape of the window function and the rate of change of the memristor state variable are defined by the parameters, D, R_{ON}, and μ_v.

In this section, to simulate the MBSSG, Biolek's window function is used [37]. Biolek window function is current-dependent and it is given as

$$f(x) = \begin{cases} 1 - (x - 1)^{2p} & , \quad i(t) \leq 0 \\ 1 - (x)^{2p} & , \quad i(t) > 0 \end{cases} \tag{8}$$

Submitting Eq. (8) into Eq. (5), it turns into

$$\frac{dx}{dt} = \frac{\mu R_{on} i(t)}{D^2} \begin{cases} 1 - (x - 1)^{2p} & , \quad i(t) \leq 0 \\ 1 - (x)^{2p} & , \quad i(t) > 0 \end{cases} \tag{9}$$

The input current of the MBIA is also equal to the memristor current. Its output voltage is

$$V_{out} = -\frac{R(x) + R_s}{R_1} V_{in} = -\frac{(R_s + R_{OFF} - (R_{OFF} - R_{ON})x(t))}{R_1} V_{in} \tag{10}$$

The MBSSG circuit is modelled and simulated using LTspice. The circuit elements whose parameters are given in Tables 1 and 2 are used for its simulation. Biolek memristor model parameters, which give similar and the closest hysteresis curves to the experimental ones given in Figure 2, are used in the simulations and given in Table 1. More information about Biolek model can be found in [37]. LM358 opamp is chosen due to the fact that it is cheap and easy to find. The input resistance of the inverting amplifier is chosen 560 KΩ high enough to limit the current of the Carbon-based memristor to prevent its destruction. Normally, in [32], a protection resistor between 50 and 100 KΩ is suggested to be used in series with the carbon-based memristor but a 47 KΩ resistor is used as the protection resistor since the memristor current is already limited with the high-value input resistor.

A memristor must have three fingerprints: a) it must have zero-crossing frequency-dependent pinched hysteresis curves, b) With increasing frequency, the area of its hysteresis curve should decrease, and c) At very high frequencies, it should turn into a single value function. Simulated hysteresis loops of the memristor model are given in Figure 4 and it shows the three fingerprints. The frequencies are chosen as monotonously increasing to illustrate that the memristor model has all the needed fingerprints. Both the parameters of the memristor model given in Table 1 and operation frequencies define the shape of the memristor's hysteresis loop.

Table 1. Memristor model parameters

Parameter	Symbol	Value
Minimum memristance or resistance of the memristor	R_{ON}	125 KΩ
The memristor maximum memristance or resistance	R_{OFF}	1250 KΩ
The dopant mobility	μ	40.10-14 m^2/V.s
Physical length of the memristive element	D	10 nm
Power parameter of the Biolek window function	p	2

Table 2. The components used in the MBSSG

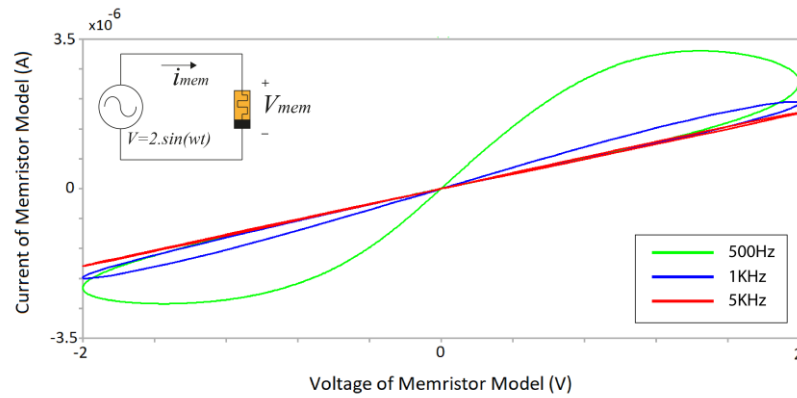| Device	Symbol	Value
Resistance of Protection Resistor	R_s	47 KΩ
Input Resistance of Inverting Amplifier	R_1	560 KΩ
Opamp	*Op1, Op2*	LM358

Figure 4. *Hysteresis Loops of memristor model for 0.5, 1, and 5 kHz*

The sawtooth signal generator is simulated for several different frequencies using the model. The simulation results of the MBSSG are shown in Figures 5. Its output voltage is not symmetric due to the asymmetric current dependency of the Biolek window function. If a memristor's memristance value takes its minimum or maximum value and stays constant even though a current flows through it and its polarity does not change, the memristor is said to be in saturation. The time in which a memristor switches its resistance from its minimum value to its maximum value or from its maximum value to its minimum value is called the memristive or resistive switching time. At low frequencies, the memristor saturates since the electrical half period is higher than memristive or resistive switching time and memristance takes its minimum and/or maximum value in an electrical period. Its output voltage is almost trapezoidal at 50 kHz since an alternance is higher than the resistive switching time, the Knowm memristor becomes saturated as shown in Figure 5a. MBIA input current is almost trapezoidal and can be considered to be almost constant in each alternance. The output voltage of the MBSSG is almost trapezoidal at 50 kHz due to the fact that the memristor gets saturated at low frequencies which can be seen from the intervals in which the output voltage stays constant as shown in Figure 5a. The output voltage resembles more to a sawtooth waveform than a trapezoidal waveform at 100 kHz as shown in Figure 5b. Both of the output voltages are sawtooth waveform as shown in Figures 5c and 5d. The result of the simulations given here shows that the sawtooth-signal generator produces a nice-looking sawtooth signal at the frequency range from 150 kHz to 500 kHz.
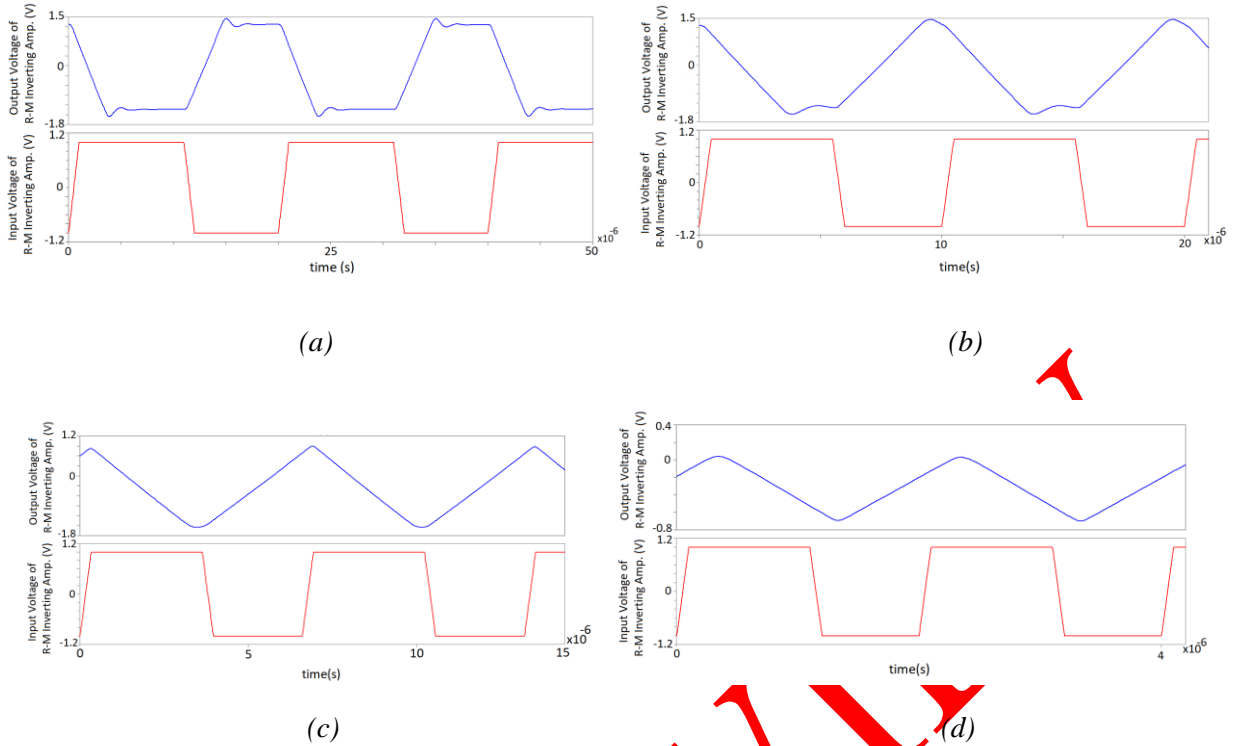
(a)

(b)

(c)

(d)

Figure 5. *Input and output voltages of the MBSSG for a) 50, b) 100, c) 150, and d) 500 kHz*

4. EXPERIMENTAL RESULTS

LM358 operational amplifiers are used in the signal generator shown in Figure 3. The circuit is mounted on a protoboard, and experiments are performed. LM358 operational amplifiers are used in the circuit. The experimental waveforms given in Figure 6 are acquired.
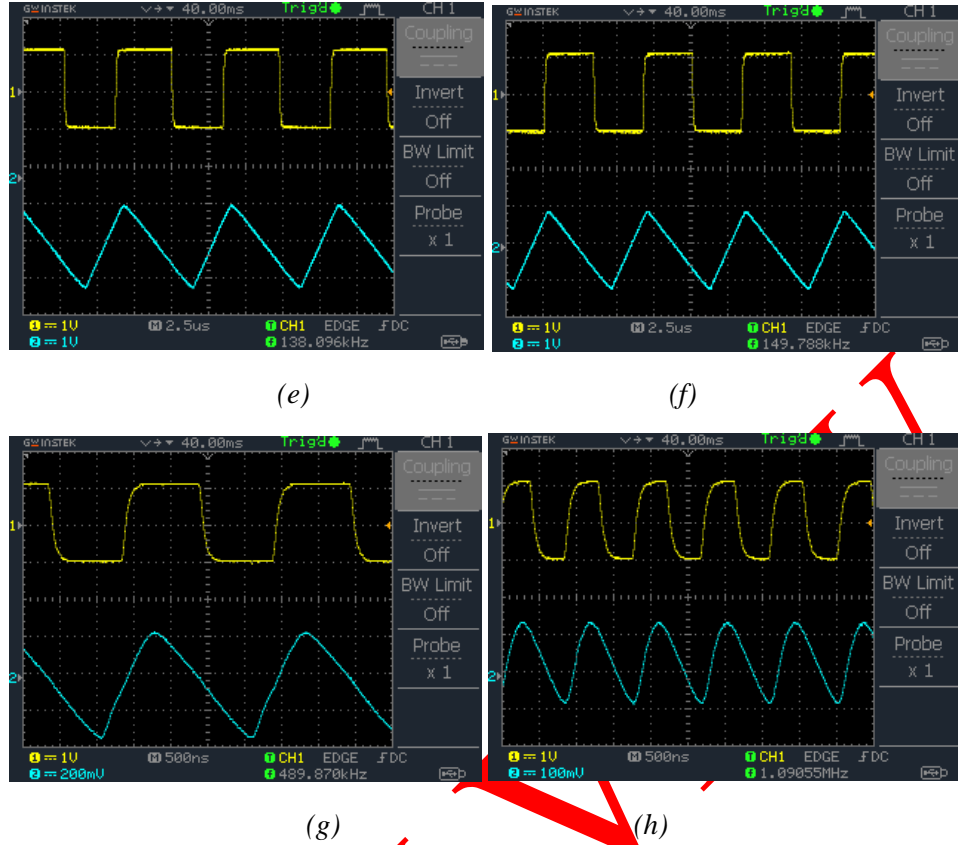

(a)

(b)

(c)

(d)

(e) *(f)*

(g) *(h)*
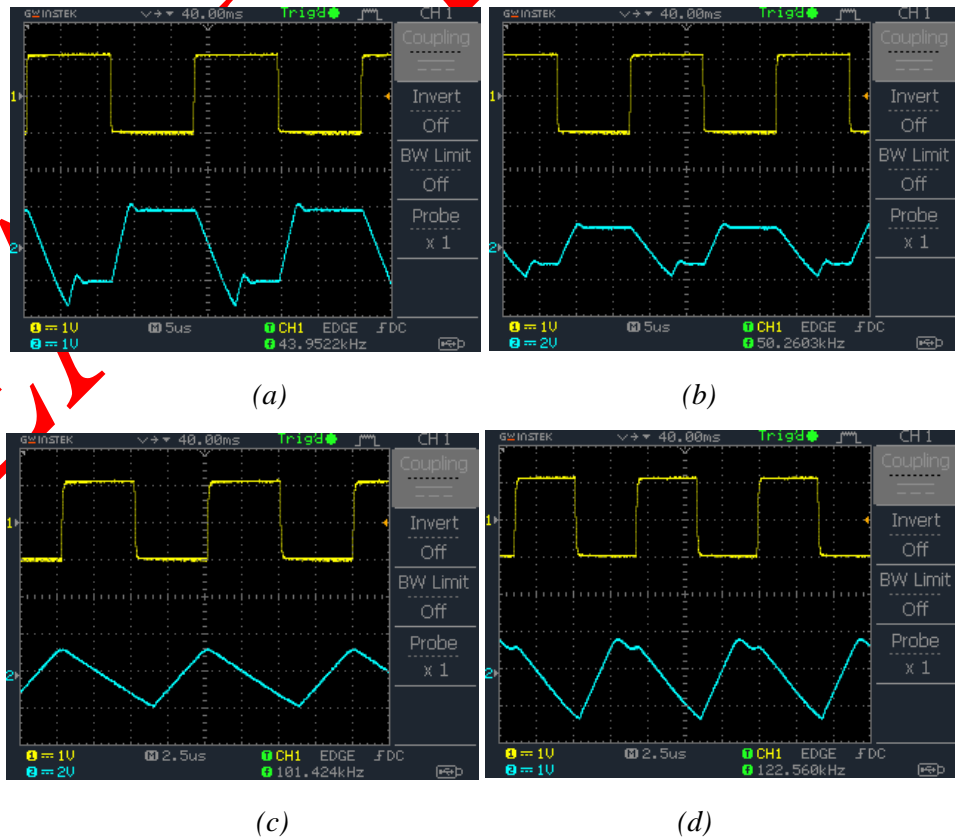
Figure 6. *Signal Generator Input and Output Voltages*

The rise times, the fall times, and the amplitude values of the generated output signal of the MBSSG circuit obtained from Figure 6 have been given in Table 3. As seen from Table 3, under 100 kHz, the rise time is almost constant and around 2.1 µs, the rise time is also almost constant and around 2.6 µs between 100 kHz and 200 kHz, the rise time falls down with increasing frequency above 100 kHz. The fall time is not monotonous, it varies with respect to time, and it is hard to find a region in which it can be regarded as almost constant. The positive peak voltage values are constant below 100 kHz while the negative peak voltage values are almost constant. The positive peak voltage value becomes maximum and the negative peak voltage value becomes (mathematically) minimum at 101.42 kHz. At 122.56 kHz, the positive peak voltage value decreases and the negative peak voltage values increases. Between 138.09 kHz and 149.78 kHz, both the positive and the negative peak voltage values keep increasing. At and above 489.87 kHz, the positive peak voltage values fall down significantly. At 489.87 kHz, the negative peak voltage value takes a very (mathematically) high value, and at 1.09 MHz, the negative peak voltage value falls down again. The variation of the negative peak voltage value is not monotonous. There occurs an unexpected phase difference at frequencies above 149.78 kHz that can be explained by the existence of either the opamp's or the Carbon-based memristor's capacitive behavior. The triangular waveform is given as a special case of the sawtooth waveform in the literature. If its fall time is equal to its rise time, a sawtooth waveform turns into a triangular waveform. According to the experimental results, the fall time and the rise time are never equal to each other as can be seen in Table 3. That's why, according to the literature, the signal generator's waveforms can be called sawtooth waveforms.

***Table 3.** Some properties of the output signal the MBSSG*

Frequency	Rise Time	Fall Time	The Positive Peak Voltage Value	The Negative Peak Voltage Value
43.95 kHz	2.2 μs	3.8 μs	1.3V	-1.6V
50.26 kHz	2.1 μs	5.6 μs	1.3V	-1.7V
101.42 kHz	2.1 μs	6.5 μs	1.5V	-1.8V
122.56 kHz	2.7 μs	5.5 μs	0.9V	-1.3V
138.09 kHz	2.6 μs	4.7 μs	1.0 V	-1.2 V
149.78 kHz	2.5 μs	4.1 μs	1.1V	-1.1V
489.87 kHz	0.67 μs	1.35 μs	0.22V	-0.32V
1.09 MHz	0.32 μs	0.6 μs	0.14V	-0.75V

At low frequencies, memristor saturates, i.e., the electrical half period is higher than memristive or resistive switching time and memristance takes its minimum. Memristor saturation can be seen in Figures 6a and 6b. In these cases, the output waveform is not a sawtooth waveform. The output waveforms which resemble a sawtooth wave most are shown in Figures 6c and 6g.

In [31], it was claimed that output waveform of the MBSSG can be optimized selecting its circuit parameters properly. Using the Knowm memristor and the circuit parameters given in Table 2, the best-looking sawtooth waveforms at the output is obtained in the range of 100-350 kHz as they can be seen in from Figures 6c through 6g. The sawtooth output is similar for both simulated and experimental cases under 350 kHz. However, above 350 kHz the experimental behavior deviates from the simulated behavior. At Figure 6d, there is a strange ripple in output voltage that it is also predicted by the simulations. A similar ripple is also predicted by the simulations at 50 kHz and can be seen in Figure 5b. The ripple may result from the nonlinear dopant drift within the memristor, and it is predicted that it depends on the due to the power parameter in the Biolek's window function. Output voltage of the generator does not always resemble a sawtooth waveform. Due to the simulations given in [29,30], it was expected that it would look like a square waveform while the operation frequency increases. However, the experiments showed that if the frequency gets around 1 MHz, then, the output waveform turns into a smoothened sawtooth waveform as shown in Figure 6h and therefore the output cannot be called a sawtooth waveform anymore. This phenomenon can be seen in Tablo 3. At frequencies 489.87 kHz and 1.09 MHz rising time, falling time, output voltage of the signal generator is relatively low. In this case, it looks more like output voltage ripple of a rectifier with a DC offset which makes it have negative voltage values, too. We have found two reasons for it: a) the bandwidth of the used opamp and b) the carbon-based memristor also behaves as an R-C circuit at high frequencies and the capacitive effects are perhaps the main reason for tapering, which will be addressed more in a future study. The simulations done in this study show that the memristor model predicts the generator behavior well at the frequencies up to 350 kHz. However, the simulations are not able to predict the experimental behavior for frequencies above 350 kHz. Therefore, there is a need for better carbon-based memristor models especially for high frequencies. It may also be possible to utilize the capacitive effects are to shape the output waveforms.

5. CONCLUSION

In [30,31], it is claimed that a MBSSG can be made. The MBSSG given in [30,31] is examined experimentally using a carbon-based memristor in this study. The MBSSG is simulated with LTspice. The simulated and experimental MBSSG waveforms are compared. It has been inferred that the MBSSG waveforms behave differently than the simulation results given in [29,30] using the system model with Biolek's window functions predicts. Also, the experiments have shown that a nice-looking sawtooth wave is obtained at frequencies as high as 400 kHz even though the waveform is tapered a bit.

In [31], it has been claimed that, when memristor is out in the markets, it becomes feasible to make MBSSG circuits and, if the new component is mismodeled, this causes its application circuits also mismodeled. The experimental study revealed the prediction as true. For example, the rise time, the fall time, and the peak

voltage values of the output signal vary in unexpected ways by operation frequency over 150 KHz. Such a thing maybe indicating that there are capacitive effects either due to the opamp or the memristor. We suggest that a MBSSG performance should always be examined experimentally while designing one until the memristor models get matured enough. For this reason, the companies which aim to make memristors marketable should also provide their models describing them accurately to ease their usage in such generators. In the literature, to the best of our knowledge, there is not any carbon-based memristor model with explicit mathematical equations and parameters in which the capacitive effects are considered for the carbon-based memristors. In [38] and [39], equivalent circuits for Carbon- and Tungsten- based memristor topologies are suggested and it is predicted that the nonlinear capacitive effects can perhaps be of memcapacitive nature, but a methodology is not given for how to calculate the capacitive effects. There is a need for better Carbon-based memristor models which take capacitive effects into account, especially for high-frequency operation regions. Such a model may include a nonlinear capacitor or a memcapacitor connected in parallel with a memristive element. The charge of the nonlinear capacitor or the memcapacitor may be an additional state variable in such a model. Also, a methodology must be given for obtaining the capacitor parameters of the needed model. Such a methodology may be more complex than the one given for memristors [40] but it may be a starting point. If the capacitive effects are found to be the main reason for the tapering of the waveform, they can be used to modify the output waveforms for the best performance in the future.

ACKNOWLEDGEMENT

CONFLICTS OF INTEREST

No conflict of interest was declared by the authors.

REFERENCES

[1]   Chua, L. O., "Memristor - The Missing Circuit Element", IEEE Transactions on Circuit Theory, 18: 507-519, (1971).

[2]   Chua, L. O., Kang, S. M., "Memristive devices and systems", Proceedings of the IEEE, 64(2): 209-23, (1976).

[3]   Strukov, D. B., Snider, G. S., Stewart, D. R., Williams, R. S., "The missing memristor found", Nature (London), 453: 80-83, (2008).

[4]   Williams, S., "How we found the missing memristor", IEEE Spectrum, 45(12): 28–35, (2008).

[5]   Kavehei, O., Iqbal, A., Kim, Y.S., Eshraghian, K., Al-Sarawi, S. F., Abbott, D., "The Fourth Element: Characteristics, Modelling, and Electromagnetic Theory of the Memristor", Proceedings of Royal Society A, 466(2120): 2175-2202, (2010).

[6]   Mazumder, P., Kang, S. M., Waser, R., "Memristors: devices, models, and applications", Proceedings of the IEEE, 100(6): 1911-1919, (2012).

[7]   Hu, S. G., Wu, S. Y., Jia, W. W., Yu, Q., Deng, L. J., Fu, Y. Q., Chen, T. P., "Review of nanostructured resistive switching memristor and its applications", Nanoscience and Nanotechnology Letters, 6(9): 729-757, (2014).

[8]   Pershin, Yu V., Martinez-Rincon, J., Di Ventra, M., "Memory circuit elements: from systems to applications", Journal of Computational and Theoretical Nanoscience, 8(3): 441-448, (2011).

[9]   Prodromakis, T., "Two centuries of memristors", In Chaos, CNN, Memristors and Beyond: A Festschrift for Leon Chua with DVD-ROM, composed by Eleonora Bilotta, 508-517, (2013).

[10]   Pershin, Y. V., Di Ventra, M., "Practical approach to programmable analog circuits with memristors", IEEE Transactions Circuits and Systems I: Regular Papers, 57(8): 1857–1864, (2010).

[11]   Toumazou, T. C., "A Review on Memristive Devices and Applications", 17th IEEE International Conference on Electronics, Circuits, and Systems (ICECS), 934 – 937, (2010).

[12]   Shin, S., Kim, K., Kang, S. M., "Memristor-based fine resolution programmable resistance and its applications", in ICCCAS 2009 International Conference on Communications, Circuits and Systems, 948–951, (2009).

[13]   Vaidyanathan, S., Volos, C. (Eds.)., "Advances in memristors, memristive devices and systems" (Vol. 701). Springer, (2017).

[14]   Rakitin, V. V., Rusakov, S. G., "Memristor based Oscillators with Controlled Threshold Parameters", In 2020 European Conference on Circuit Theory and Design (ECCTD), IEEE, 1-4, (2020).

[15]   Zidan, M. A., Omran, H., Smith, C., Syed, A., Radwan, A. G., Salama, K. N., "A family of memristor-based reactance-less oscillators", International Journal of Circuit Theory and Applications, 42(11): 1103-1122, (2014).

[16]   El-Naggar, A. M., Fouda, M. E., Madian, A. H., Radwan, A. G., "Reactance-less RM relaxation oscillator using exponential memristor model", In 2016 28th International Conference on Microelectronics (ICM), IEEE., 361-364, (2016).

[17]   Rakitin, V. V., Rusakov, S. G., "Operating principles of reactance-less memristor-based oscillators", Journal of Communications Technology and Electronics, 62(6): 621-625, (2017).

[18]   Rakitin, V. V., Rusakov, S. G., "Principles of the Functioning of Nonreactive Double Memristor Oscillators", Journal of Communications Technology and Electronics, 64(6): 622-628, (2019).

[19]   Bodo, B., Fouda, J. A. E., Mvogo, A., Tagne, S., "Experimental hysteresis in memristor based Duffing oscillator", Chaos, Solitons & Fractals, 115: 190-195, (2018).

[20]   Sabarathinam, S., Volos, C. K., Thamilmaran, K., "Implementation and study of the nonlinear dynamics of a memristor-based Duffing oscillator", Nonlinear Dynamics, 87(1): 37-49, (2017).

[21]   Varshney, V., Sabarathinam, S., Prasad, A., Thamilmaran, K., "Infinite number of hidden attractors in memristor-based autonomous duffing oscillator", International Journal of Bifurcation and Chaos, 28(01): 1850013, (2018).

[22]   Mutlu, R., "Solution of TiO2 memristor-capacitor series circuit excited by a constant voltage source and its application to calculate operation frequency of a programmable TiO2 memristor-capacitor relaxation oscillator", Turkish Journal of Electrical Engineering & Computer Sciences, 23(5): 1219-1229, (2015).

[23]   Mosad, A. G., Fouda, M. E., Khatib, M. A., Salama, K. N., Radwan, A. G., "Improved memristor-based relaxation oscillator", Microelectronics Journal, 44(9): 814-820, (2013).

[24]   Fouda, M. E., Radwan, A. G., "Power dissipation of memristor-based relaxation oscillators", Radioengineering, 24(4): 968-973, (2015).

[25]   Talukdar A, Radwan AG, Salama KN., "Generalized model for memristor-based Wien-family oscillators," Journal of Microelectronics, 42: 1032–1038, (2011).

[26]   Bao, H., Wang, N., Wu, H., Song, Z., Bao, B., "Bi-stability in an improved memristor-based third-order Wien-bridge oscillator", IETE Technical Review, 36(2): 109-116, (2019).

[27]   Rajagopal, K., Li, C., Nazarimehr, F., Karthikean, A., Duraisamy, P., Jafari, S., "Chaotic dynamics of modified wien bridge oscillator with fractional order memristor", Radioengineering, 28(1): 165-174, (2019).

[28]   Wang, N., Bao, B., Jiang, T., Chen, M., Xu, Q., "Parameter-independent dynamical behaviors in memristor-based Wien-bridge oscillator", Mathematical Problems in Engineering, (2017).

[29]   Abuelma'atti, M. T., Khalifa, Z. J., "A memristor-based Wien-bridge sinusoidal/chaotic oscillator", International Journal of Electrical Engineering Education, 53(3): 280-288, (2016).

[28]   Wey, T. A., Benderli, S., "Amplitude modulator circuit featuring TiO2 memristor with linear dopant drift", Electronics Letters, 45: 1103 – 1104, (2009).

[30]   Özgüvenç A., Mutlu R., Karakulak E., "Sawtooth signal generator with a memristor," 1st International Conference on Engineering Technology and Applied Sciences, (2016).

[31]   Kurtdemir, A., Mutlu, R., "Modeling and Simulation of a Memristor-Based Sawtooth Signal Generator Using Nonlinear Dopant Drift Memristor Models", European Journal of Engineering and Applied Sciences, 2(1): 44-57, (2019).

[32]   Knowm Self Directed Channel Memristors, https://knowm.org/downloads/Knowm_Memristors.pdf Access date: 10.04.2020

[33]   HP   Hynix   to   Collaborate   on   Memristor   Memory   Technology, https://www.informationweek.com/desktop/hp-hynix-to-collaborate-on-memristor-memory-technology/d/d-id/1092114 Access date: 01.04.2020

[34]   Volos, C., Nistazakis, H., Pham, V. T., Stouboulos, I. "The First Experimental   Evidence of Chaos from a Nonlinear Circuit with a Real Memristor", In 2020 9th International Conference on Modern Circuits and Systems Technologies (MOCAST) 1-4, IEEE, September, (2020).

[35]   Adhikari, S. P., Sah, M. P., Kim, H., Chua, L. O., "Three fingerprints of memristor", IEEE Transactions on Circuits and Systems I: Regular Papers, 60(11): 3008-3021, (2013).

[36]   Wey, T. A., Jemison, W. D., "Variable gain amplifier circuit using titanium dioxide memristors", IET Circuits, Devices & Systems, 5: 59–65, (2011).

[37]   Biolek, Z., Biolek, D., Biolkova, V., "SPICE model of memristor with nonlinear dopant drift", Radioengineering, 18(2): 210–214, (2009).

[38]   Dalmış, C, "Examination of polarity-dependent charging and discharging of capacitor circuits containing Carbon and Tungsten based memristors," Tekirdağ Namık Kemal University, Institute of Natural and Applied Sciences, Master's Thesis, (2021).

[39]   Dalmış, C., Mutlu, R., Karakulak, E., "Existence of Capacitive Effects in a Tungsten-Based SDC Memristive System", Informacije MIDEM, 53(3): (2023).

[40]   Mutlu, R., Karakulak, E., "A methodology for memristance calculation", Turkish Journal of Electrical Engineering and Computer Sciences, 22(1): 121-131, (2014).